Unidirectional perfect magnetic metamaterial absorber based on nonreciprocal mie resonance

Jingjing Yu (余晶晶)[1*], Huajin Chen (陈华金)[1,2], Xinning Yu (俞昕宁)[1], and Shiyang Liu (刘士阳)[1,2]

[1]*Institute of Information Optics, Zhejiang Normal University, Jinhua 321004, China*
[2]*State Key Laboratory of Surface Physics, Department of Physics (SKLSP), Fudan University, Shanghai 200433, China*
*Corresponding author: minior@qq.com

In present work, we demonstrate that when a transverse magnetic (TM) Gaussian beam is incident to a magnetic metamaterial (MM) slab, it can be completely absorbed at a particular direction, resulting in a unidirectional perfect absorption. The unidirectionality is due to the time reversal symmetry (TRS) breaking nature of the MM; while the perfect absorbing effect is explained by the multiple scattering theory and the effective medium theory. By tuning the magnitude and the orientation of the external magnetic field, the working frequency can be adjusted and the unidirectionality can be reversed. Accordingly, we can design tunable compact optical devices to achieve unidirectional perfect absorption.

OCIS codes: 130.4815, 160.3918, 240.6680.
doi: 10.3788/COL201412.S11301.

During recent decades, metamaterials, made up of specified subwavelength resonant building blocks, have attracted increasing interest due to exotic properties and fascinating potential application[1,2]. One of typical paradigms are perfect absorber[3], the working frequency, which ranges from microwave[4,5] (terahertz)[6–8] to infrared[9–11], and even optical region[12,13], and the working angle can be a single direction[3,14], a wide angle[15–17] and even an omni-direction[18–21]. Due to the flexible external tunability by an external magnetic field (EMF), the magnetic metamaterial (MM) based absorber can be more desirable for practical applications. In addition, the time reversal symmetry (TRS) is broken for the MM under the exertion of an EMF[22–24], enabling it to work unidirectionally.

In this work, we designed a ferrite based unidirectional perfect MM absorber[25]. Then by calculating the transmission as the function of the incident angle and working frequency, the scattering phase shift of the n–th angular momentum channel (AMC), and effective constitutive parameters, we present the simulated unidirectional perfect absorbing effect. The results show that the origin of the unidirectional absorbing effect relies on the TRS breaking characteristic of the ferrite materials under an EMF and the nonreciprocal Mie resonance. Furthermore, the unidirectionality and the working frequency can be manipulated flexibly with an EMF, which makes the designed absorber much easier to meet the requirements of the practical applications.

To study the unidirectional perfect absorbing effect, a ferrite material with a strong loss is necessary. In our work, we have used Ni–Zn ferrite with large damping coefficient, whose magnetic permeability is a second-rank tensor in the form[26]

$$\hat{\mu} = \begin{pmatrix} \mu_r & -i\mu_k & 0 \\ i\mu_k & \mu_r & 0 \\ 0 & 0 & 1 \end{pmatrix}, \tag{1}$$

with

$$\mu_r = 1 + \frac{f_m(f_0 - i\alpha f)}{(f_0 - i\alpha f)^2 - f^2}, \quad \mu_k = \frac{f_m f}{(f_0 - i\alpha f)^2 - f^2},$$

where $f_m = \frac{1}{2\pi}\gamma M_s$ is the characteristic frequency with the gyromagnetic ratio $\gamma = 2.8$ MHz/Oe, $M_s = 2350$ Gauss is the saturation magnetization of the Ni–Zn ferrite, $f_0 = \frac{1}{2\pi}\gamma H_0$ is the resonance frequency with H_0 being the sum of the EMF applied in z direction and the shape anisotropy field. For the Ni–Zn ferrite rods, the permittivity is $\varepsilon_s = 12.7(1 + i4 \times 10^{-4})$, and the damping coefficient is $\alpha = 6 \times 10^{-2}$.

The magnetic metamaterials (MM) considered in present work consist of an array of Ni–Zn ferrite rods arranged periodically as a square lattice in the air, where the lattice constant is $a = 7.05$ mm and the radius of the ferrite rod is $r = 2.25$ mm. We observed the phenomenon when a transverse magnetic (TM) Gaussian beam with electric field polarized along z direction incident on a 5-layer MM slab from two symmetrically opposite directions $\theta_{inc} = \pm 60°$. The working frequency is $f = 4.35$ GHz, and the EMF is $H_0 = 500$ Oe oriented along z direction, parallel to the rod axis. The results are shown in Fig. 1, where we can find that the Gaussian beam incident from left hand side with the incident angle $\theta_{inc} = 60°$ is completely absorbed, while the reflectance and transmittance is nearly vanished as shown in panel (a). In this case, the slab behaves as a perfect
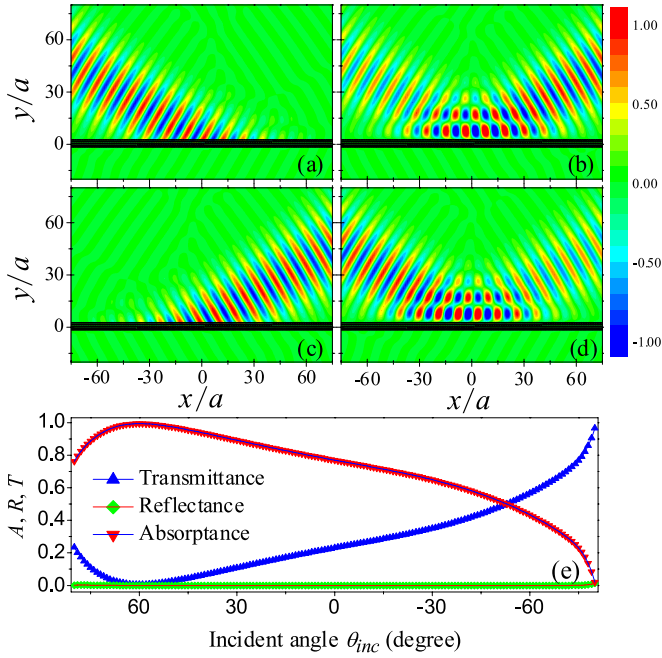
Fig. 1. The electric field patterns for a TM Gaussian beam incident from two symmetrically opposite directions with the incident angle equal to 60° (a) and –60° (b). Panels (c) and (d) are the same as panels (a) and (b) except that the magnetization is reversed. (e) The absorptance, reflectance, and transmittance are plotted as the functions of the incident angle θ_{inc} in (c). The metamaterial is made up of an array of Ni–Zn ferrite rods in square lattice with lattice space $a = 7.05$ mm and the rod radius $r = 2.25$ mm. The EMF satisfies $H_0 = 500$ Oe.

metamaterial absorber. Differently, for the Gaussian beam incident from a symmetrically opposite direction with $\theta_{inc} = -60°$, the EM energy is obviously reflected, as can be observed from panel (b). That is to say, the designed absorber based on ferrite materials can be operated unidirectionally. This nonreciprocity enables the absorber possess switch characteristic, which makes it more useful for the implementation of microwave devices. We also calculated the absorptance (A), reflectance (R), and transmittance (T) as the functions of the incident angle θ_{inc}, the results are shown in panel(e), where red down triangle, blue up triangle, and green diamond mark, respectively, A, R, and T. At the incident angle $\theta_{inc} = 60°$ the absorptance equals to 1 and at symmetrically opposite direction $\theta_{inc} = -60°$, an obvious reflectance $R = 0.57$ can be observed, which coincident with Figs. 1(a) and (b). In addition, although the perfect absorbing effect can be realized only in a very narrow angle around $\theta_{inc} = 60°$, for the practical application, we can rotate the device around the central axis to make it operable for any beam direction.

The unidirectional phenomenon relies on the TRS breaking characteristic of the ferrite materials under an EMF, absent for the ordinary dielectric and metallic materials. To illustrate this point, we can control the nonreciprocity by reversing the orientation of magnetization from z to $-z$, still parallel to the rod axis. The simulation results are shown in Figs. 1(c) and (d)

where we can find that by reversing the EMF the perfect absorbing effect is realized at the symmetrically opposite direction with $\theta_{inc} = -60°$, while at $\theta_{inc} = 60°$, an obvious reflection beam is observed. The electric field patterns are mirrored compared to those in Figs. 1(a) and (b). Accordingly, the unidirectionality is the consequence of the TRS breaking and can be reversed by an EMF.

To explore the origin of the unidirectional absorbing effect in more detail, we also calculate A, R, and T as the functions of frequency, as indicated by the black, red, and blue lines, respectively, for the direction of EMF along $\pm z$, respectively, as indicated by the solid and dashed lines in Fig. 2(a). It can be found that for the EMF along z direction the best operating frequency is located at $f = 4.35$ GHz, where the absorptance is equal to 1, while an obvious reflectance equal to nearly 0.57 occurs when the EMF is reversed to $-z$ direction. This remarkable difference relies on the TRS breaking characteristic of the ferrite materials under an EMF, which is consistent with the electric field patterns in Fig. 1. All the electric field patterns and transmissivity are calculated by employing the multiple scattering method[27] based on Mie scattering theory. The Mie scattering coefficient b_n can be written as $b_n = -1/(1 + i\cot\eta_n)$, where η_n is the scattering phase shift of the n–th AMC. The tangent of
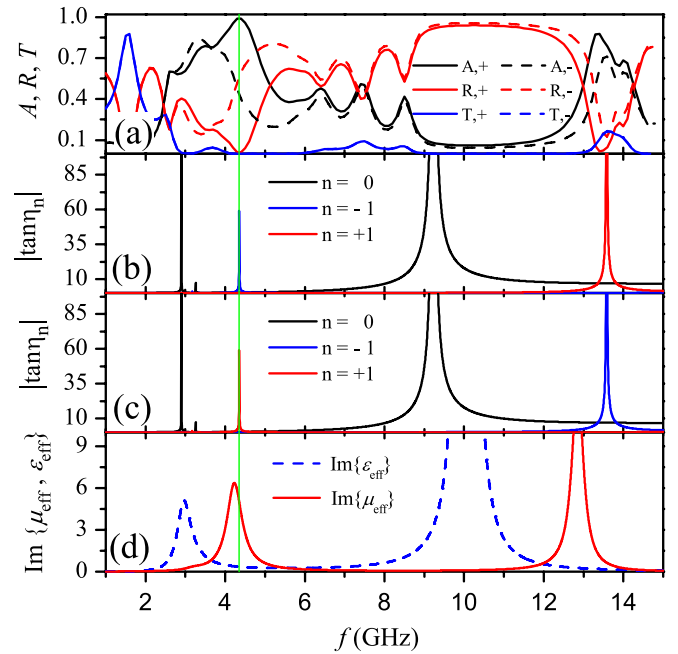

Fig. 2. (a) The absorptance, reflectance, and transmittance are plotted as the functions of the frequency for two opposite EMF directions $\pm z$ and the beam incident angle $\theta_{inc} = -60°$. The tangent of scattering phase shift $|\tan\eta_n|$ versus frequency for two opposite EMF directions, z and $-z$, are shown in panels (b) and (c), respectively. (d) The peaks denote the 0th and $\pm$1st AMC resonances. (d) The imaginary parts of the effective magnetic permeability μ_{eff} and effective permittivity ε_{eff} of the MM versus the frequency. The other parameters are the same as those in Fig. 1.

the scattering phase shift $|\tan\eta_n|$ versus frequency are shown in Figs. 2(b) and (c), respectively, for a Ni-Zn ferrite rod of the radius $r = 2.25$ mm under two opposite magnetization. The peaks corresponds to the Mie resonance of a single rod at different AMCs. The –1st AMC resonance corresponds to the absorption peak for the EMF along z direction as shown in panel (a). Then, by reversing the magnetization along $-z$ direction the +1st AMC resonance is excited at the same frequency, but the absorption is only about 0.43. Actually, this +1st AMC resonance induces the perfect absorption for the beam incident from the symmetrically opposite direction with $\theta_{inc} = -60°$. The sharp difference for the –1st AMC resonance and the +1st AMC resonance arises from the TRS breaking nature of the ferrite materials under an EMF, resulting in the nonreciprocity of the MM. In the long wavelength limit, we can retrieve the effective constitutive parameters of the MM within the effective-medium theory (EMT)[28], which is helpful for the understanding of the unidirectional perfect absorption and the resonant behavior. In Fig. 2(d), we present, respectively, the imaginary parts of the effective permittivity ε_{eff} and the effective magnetic permeability μ_{eff}, as indicated by the blue dashed line and red solid line. It can be found that at the working frequency $f = 4.35$ GHz, a large value of $\mathrm{Im}(\mu_{eff})$ greater than 5 can be realized. This suggests that the TM Gaussian beam is coupled to the –1st AMC resonance entirely for the incident angle $\theta_{inc} = 60°$ and then consumed completely due to strong loss, leading to the unidirectional perfect absorption.

Finally, we increase H_0 from 500 Oe to 1080 Oe, the 0-th AMC resonance replace the −1st AMC resonance at the working frequency $f = 4.35$ GHz and for the EMF along z direction. The electric field pattern is shown in Fig. 3(a), where an obvious reflected beam is observed. That is to say, the 0-th AMC resonance is independent to the unidirectional perfect absorption, but leads to strong reflection. The $|\tan\eta_n|$ under the EMF $H_0 = 1080$ Oe are calculated and presented in Fig. 3(c), where two -1st AMC resonance can be observed. By choosing the second peak of -1st AMC resonance $f = 5.81$ GHz as the working frequency, we have performed the simulation. The electric field pattern is presented in Fig. 3(b), where we can find that the Gaussian beam is completely absorbed, and the reflectance and transmittance is nearly zero. Compared to the perfect absorber in previous work, one particular advantage of the MSP based metamaterial absorber is the tunability of the working frequency by an EMF.

In summary, we have designed a ferrite based unidirectional perfect metamaterial absorber with the tunable working frequency and nonreciropcity. By calculating the transmittance, the AMC resonances, and the effective constitute parameters, we can find that the unidirectional phenomenon originates from TRS breaking nature of the ferrite materials and the excitation of the +1st or –1st AMC resonance, dependent
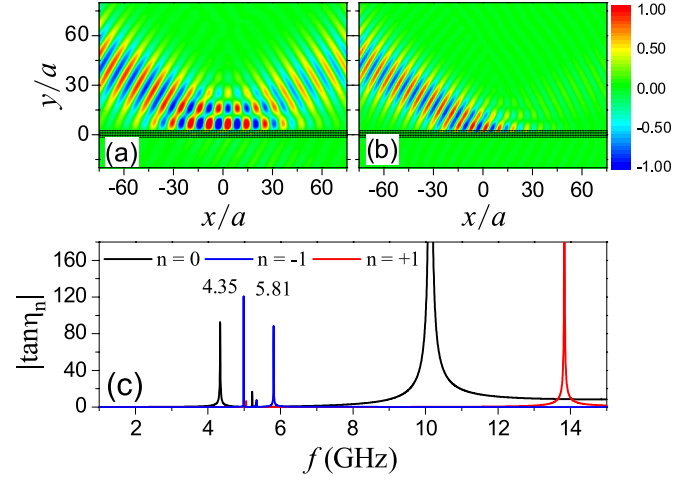

Fig. 3. The electric field patterns for a TM Gaussian beam incident from the directions $\theta_{inc} = 60°$ with the working frequency equal to $f = 4.35$ GHz (a) and $f = 5.93$ GHz (b). $|\tan\eta_n|$ are plotted as the functions of the frequency in panel (c). The EMF satisfies $H_0 = 1080$ Oe. The other parameters are same as those in Fig. 1.

on the orientation of the magnetization. In addition, the EMT indicates a large $\mathrm{Im}(\mu_{eff})$ appears, leading to the perfect absorption. More importantly, by tuning the direction and magnitude of EMF the unidirectionality and the working frequency can be flexibly controlled, which makes it more desirable for practical applications.

References

1. J. B. Pendry, Phys. Rev. Lett. **85**, 3966 (2000).
2. N. I. Zheludev, Science **328**, 582 (2010).
3. N. I. Landy, S. Sajuyigbe, J. J. Mock, D. R. Smith, and W. J. Padilla, Phys. Rev. Lett. **100**, 207402 (2008).
4. B. Zhu, Y. J. Feng, J. M. Zhao, C. Huang, and T. Jiang, Appl. Phys. Lett. **97**, 051906 (2010).
5. J. B. Sun, L. Y. Liu, G. Y. Dong, and J. Zhou, Opt. Express **19**, 21155 (2011).
6. Q. Y. Wen, Y. S. Xie, H. W. Zhang, Q. H. Yang, Y. X. Li, and Y. L. Liu, Opt. Express **17**, 20256 (2009).
7. H. Tao, N. I. Landy, C. M. Bingham, X. Zhang, R. D. Averitt, and W. J. Padilla, Opt. Express **16**, 7181 (2008).
8. D. Y. Shchegolkov, A. K. Azad, J. F. O'Hara, and E. I. Simakov, Phys. Rev. B **82**, 205117 (2010).
9. Y. Avitzour, Y. A. Urzhumov, and G. Shvets, Phys. Rev. B **79**, 045131 (2009).
10. K. B. Alici, A. B. Turhan, C. M. Soukoulis, and E. Ozbay, Opt. Express **19**, 14260 (2011).
11. J. Hendrickson, J. P. Guo, B. Y. Zhang, W. Buchwald, and R. Soref, Opt. Lett. **37**, 371 (2012).
12. J. M. Hao, J. Wang, X. L. Liu, W. J. Padilla, L. Zhou, and M. Qiu, Appl. Phys. Lett. **96**, 251104 (2010).

13. Z. Y. Fang, Y. R. Zhen, L. R. Fan, X. Zhu, and P. Nordlander, Phys. Rev. B **85,** 245401 (2012).

14. N. I. Landy, C. M. Bingham, T. Tyler, N. Jokerst, D. R. Smith, and W. J. Padilla, Phys. Rev. B **79,** 125104 (2009).

15. M. Diem, T. Koschny, and C. M. Soukoulis, Phys. Rev. B **79,** 033101 (2009).

16. B. N. Wang, T. Koschny, and C. M. Soukoulis, Phys. Rev. B **80,** 033108 (2009).

17. C. H. Wu, B. Neuner III, G. Shvets, J. John, A. Milder, B. Zollars, and S. Savoy, Phys. Rev. B **84,** 075102 (2011).

18. T. V. Teperik, F. J. Garcia de Abajo, A. G. Borisov, M. Abdelsalam, P. N. Bartlett, Y. Sugawara, and J. J. Baumberg, Nat. Photon. **2,** 299 (2008).

19. E. E. Narimanov and A. V. Kildishev, Appl. Phys. Lett. **95,** 041106 (2009).

20. Q. Cheng, T. J. Cui, W. X. Jiang, and B. G. Cai, New J. Phys. **12,** 063006 (2010).

21. S. Y. Liu, L. Li, Z. F. Lin, H. Y. Chen, J. Zi, and C. T. Chan, Phys. Rev. B **82,** 054204 (2010).

22. Z. Wang, Y. D. Chong, J. D. Joannopoulos, and M. Soljačić, Phys. Rev. Lett. **100,** 013905 (2008).

23. S. Y. Liu, W. L. Lu, Z. F. Lin, and S. T. Chui, Appl. Phys. Lett. **97,** 201113 (2010).

24. S. Y. Liu, W. L. Lu, Z. F. Lin, and S. T. Chui, Phys. Rev. B **84,** 045425 (2011).

25. J. J. Yu, H. J. Chen, Y. B. Wu, and S. Y. Liu, EPL, **100,** 47007 (2012).

26. D. M. Pozar, *Microwave Engineering,* 3rd Ed. (Wiley, New York, 2005).

27. D. Felbacq, G. Tayeb, and D. Maystre, J. Opt. Soc. Am. A **11,** 2526 (1994).

28. J. F. Jin, S. Y. Liu, Z. F. Lin, and S. T. Chui, Phys. Rev. B **80,** 115101 (2009).